Key Points:

- The solar eclipse effects on the geomagnetic field ΔH records and ionospheric plasma density are noticed along the penumbra path
- The solar eclipse penumbra path over Jicamarca caused the Equatorial Electrojet to weaken locally, possibly affecting Equatorial Ionization Anomaly development over South America
- The solar eclipse caused modifications in the sporadic E layer and F region over Jicamarca, showing evidence of the gravity wave occurrence

The 14 December 2020 Total Solar Eclipse Effects on Geomagnetic Field Variations and Plasma Density Over South America

S. S. Chen[1] [iD], L. C. A. Resende[1,2] [iD], C. M. Denardini[1] [iD], R. A. J. Chagas[1] [iD], L. A. Da Silva[1,2] [iD], J. P. Marchezi[1,2] [iD], J. Moro[2,3] [iD], P. A. B. Nogueira[4] [iD], A. M. Santos[1] [iD], P. R. Jauer[1,2] [iD], C. S. Carmo[1] [iD], G. A. S. Picanço[1] [iD], and R. P. Silva[1] [iD]

[1]National Institute for Space Research (INPE), São José dos Campos, Brazil, [2]State Key Laboratory of Space Weather, NSSC/CAS, Beijing, China, [3]Southern Space Coordination (COESU/INPE/MCTI), Santa Maria, Brazil, [4]Federal Institute of Education, Science and Technology of São Paulo (IFSP), Jacareí, Brazil

Abstract We discuss the effects in the geomagnetic field variations and ionospheric plasma density modifications caused by the Total Solar Eclipse that occurred on 14 December 2020 over the South American sector. We used ground-based magnetometer data and the Total Electron Content maps derived from the Global Navigation Satellite System to evaluate these changes. The results show that the geomagnetic field daily variation weakens between the first and last solar eclipse penumbra contact. Additionally, we observed a significant reduction of about 52.33 nT on the Equatorial Electrojet strength at Jicamarca (11.95°S, 76.88°W), where the solar obscuration reached 16.67% approximately. This behavior indicates that the solar eclipse in the equatorial region has possibly affected electric conductivities, altering the E region dynamo electric field. Consequently, it weakens the equatorial plasma fountain, affecting the Equatorial Ionization Anomaly development. Additionally, the ionospheric dynamics variations over Jicamarca during the solar eclipse event are analyzed using ionosonde data. We observe that the solar eclipse also caused a modification in the sporadic E layer and F region dynamics, indicating possible evidence of the gravity wave occurrence. Therefore, the results found here provide a better understanding of how the solar eclipse passage in the equatorial region affects the electron density in the low-latitude regions.

1. Introduction

Solar eclipses are remarkable phenomena to help investigate the atmosphere-ionosphere effects due to solar irradiance reduction. It is a fact that the solar irradiance where the eclipse shadow passes results in direct modification in temperature, pressure gradients, and electron density. One of the main effects of this phenomenon in the ionosphere is related to local ionospheric chemistry, such as the production and loss processes over the penumbra region (Rishbeth, 1970). This circumstance, in turn, also reduces ionospheric conductivities and affects the daily variation of the geomagnetic field along the eclipse path (Bowhill, 1970).

Based on these concepts, previous studies suggested that possible geomagnetic field changes can occur due to the solar eclipse (Bauer, 1902; Chapman, 1933). Chapman and Bartels (1940) pointed out that the geomagnetic field variations during those events are difficult to observe since frequent irregular changes in the geomagnetic field can coincide. However, Kato (1960) registered a decrease in the geomagnetic field horizontal component during a solar eclipse which was related to 58% decrease in the ionospheric conductivity. Since that, several studies have reported the solar eclipse effects on the geomagnetic field (Kim & Chang, 2018; Orozco and Muniz Barreto, 1993; van der Laan, 1970).

Going into a case study of particular solar eclipse events, Korte et al. (2001) performed a case study of the solar eclipse on 11 August 1999. They registered no evidence of the eclipse effect in geomagnetic records on the European sector. In contrast, Özcan and Aydoğdu (2004) registered that the westward component of the geomagnetic field was more affected by the same eclipse over a midlatitude region, Elazig-Turkey (39°N, 40°E).

A general overview of the averaged ground-based geomagnetic field records of 39 solar eclipse events from 1991 to 2016 is shown by Kim and Chang (2018). The authors noticed that the solar eclipse effects are most evident in the midlatitude (±30°–50° MLAT), compared to equatorial-low latitude (±0°–30° MLAT) and high latitude (±50°–90° MLAT) regions. The general aspect observed was an increase in the *Y* component and a decrease in

Writing – original draft: S. S. Chen, L. C. A. Resende
Writing – review & editing: S. S. Chen, L. C. A. Resende, C. M. Denardini, R. A. J. Chagas, L. A. Da Silva, J. P. Marchezi, J. Moro, P. A. B. Nogueira, A. M. Santos, P. R. Jauer, C. S. Carmo, G. A. S. Picanço, R. P. Silva

the X, Z, and F components of the geomagnetic field when the solar eclipse lasted longer than ∼141 min and the eclipse magnitude increased. The observations made by Özcan and Aydoğdu (2004) match the solar eclipse effects over midlatitude latitude.

The Total Solar Eclipse (TSE) that occurred on 14 December 2020 is a great opportunity to evaluate the effects on the geomagnetic field variations and the plasma density in South America. Recent studies have reported the observations and predictions of the atmospheric and ionospheric effects of this eclipse event (de Haro Barbás et al., 2022; Gómez, 2021; Martínez-Ledesma et al., 2020; Resende et al., 2022; Shrivastava et al., 2021). Using the SUPIM-INPE (Sheffield University Plasmasphere-Ionosphere Model-INPE) model, Martínez-Ledesma et al. (2020) first predicted the ionospheric response to the TSE that occurred on 14 December 2020. They found that the equatorial fountain transport would affect the low-latitude regions. In addition, they expected ionospheric changes in the conjugate hemisphere during this event. Gómez (2021) has reported, modeled, and interpreted the Gravity Waves (GWs) perturbations in the ionosphere to this solar eclipse along the totality path. The author detected the wave-induced phenomena on Total Electron Content (TEC) measurements near the Southern Andes in the Patagonia region and showed a good agreement between the SAMI3 ionospheric model predictions and the TEC data for this solar eclipse event. Analyzing geodetic and geomagnetic observatory data over the Patagonian region, Meza et al. (2021) also studied the ionospheric responses to this solar eclipse. In this case, it was investigated the geomagnetic field variations to this solar eclipse, something that until then had not been tackled by previous works. It was observed that the TEC varies with solar occultation, leading to a 10%–30% reduction in the TEC. They also compared the geomagnetic records with predictions based on the Ashour-Chapman model and found a good overall agreement with a delay of about 20 min between the maximum eclipse and the observations.

Shrivastava et al. (2021) in turn investigated the atmospheric GWs along the totality path over the Chilean Global Positioning System (GPS) receivers' sites on the same solar eclipse. The authors revealed a reduction of almost 20%–40% of TEC values, atmospheric GWs with ∼30–60 min, and a presence of large day-to-day variability in the background values of TEC to this eclipse.

So, this work aims to investigate the equatorial to low-latitude effects on the geomagnetic field records and the ionospheric plasma density in South American stations during the TSE on 14 December 2020. We used the ground-based magnetometer networks data and TEC maps derived from the Global Navigation Satellite System (GNSS) receivers in some stations in South America. Additionally, ionospheric dynamics variations over Jicamarca during the solar eclipse passage are analyzed using ionosonde data. Hence, we notice changes in the geomagnetic field and plasma density over the Southern hemisphere low-latitude stations that recovers to reference values a few hours after the solar eclipse. At the equatorial latitude, the EEJ ground strength significantly decreases compared to the reference daily geomagnetic field variation at Jicamarca. In the following sections, we present the methods and explanations about the solar eclipse's influence on the geomagnetic field variation and the plasma density in the ionosphere over South America.

2. Observations and Methods

2.1. The TSE and Control Days

The TSE registered on 14 December 2020 ($\sum Kp = 5$) has covered a part of the Southern area of the South American continent. The first and last contact of penumbra occurred at 13:33 UT and 18:53 UT, respectively. A careful analysis of the geomagnetic field observations has been carried out. Therefore, we have analyzed the possible solar eclipse effects on the ground-based geomagnetic field measurements.

Several authors selected the day before or next to the eclipse event to be the reference for analyzing their possible effects on the geomagnetic field observations (Korte et al., 2001; Orozco & Muniz Barreto, 1993). Here, we have selected 17 December 2020 ($\sum Kp = 1+$) as a control (or reference) day since the geomagnetic activity level is one of the quietest of the month. Figure 1 presents the magnetopause standoff distance (Rmp) (Shue et al., 1998), the solar wind dynamic pressure (Psw), and the north-south component of the interplanetary magnetic field (IMF Bz) at the Lagrangian point L1, obtained from the WIND spacecraft (Lepping et al., 1995; Ogilvie et al., 1995). This figure provides these interplanetary solar wind plasma and magnetic field parameters obtained by the NASA/GSFC/OMNIWeb (ftp://spdf.gsfc.nasa.gov/pub/data/omni/high_res_omni/modified/monthly_1min), with a 1-min average resolution. The reference day is shown in orange, 17 December 2020, and the eclipse day in red. Also, the solar radio flux index (F10.7) was 80.6 and 79.1 sfu, on 14 and 17 December, respectively. Magenta vertical lines indicate the first and last contact of solar eclipse penumbra.
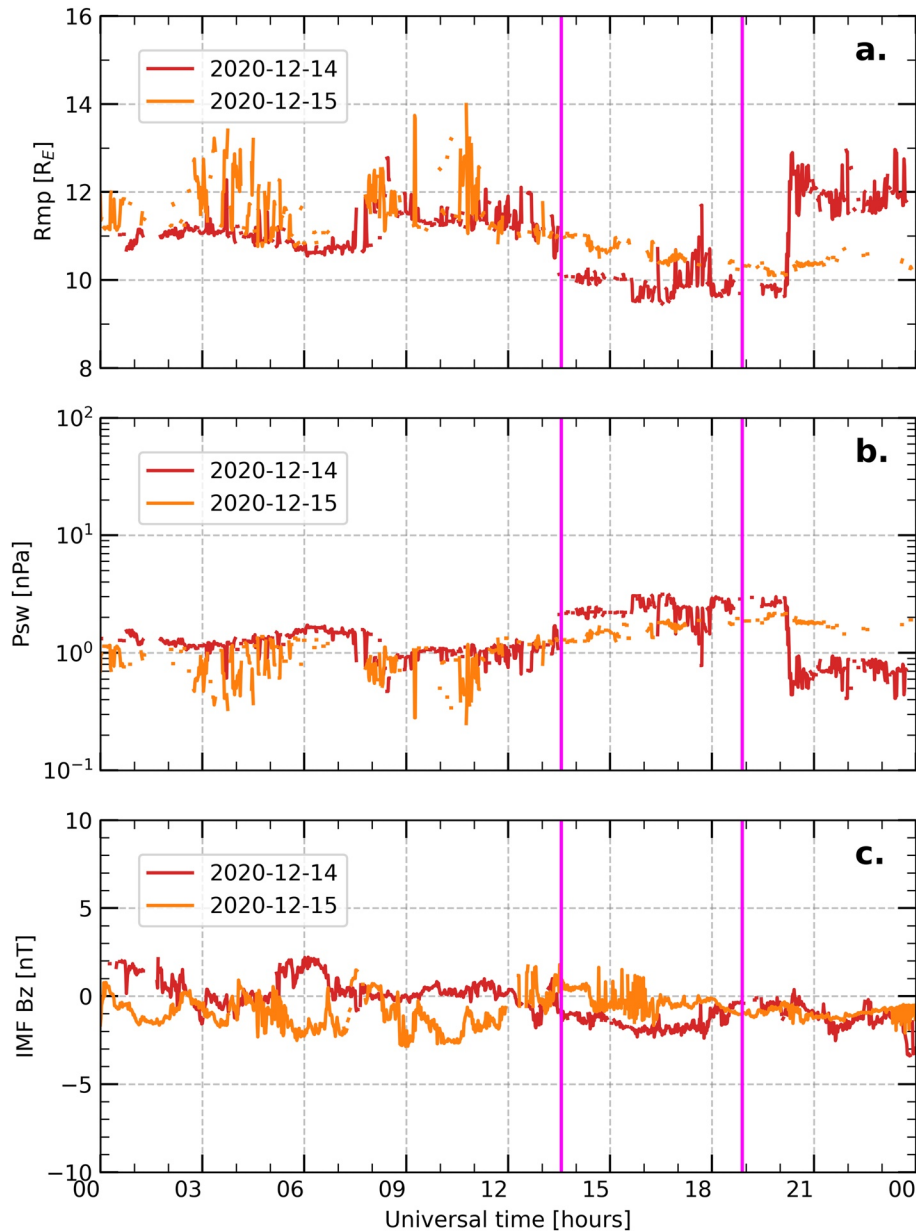
Figure 1. The interplanetary solar wind parameters measured by WIND spacecraft: (a) the magnetopause standoff distance (or *Rmp*), (b) the solar wind dynamic pressure (or *Psw*), and (c) IMF *Bz* component, during the eclipse day (red) and the control day (orange). Magenta vertical lines indicate the first and last contact of solar eclipse penumbra.

The interplanetary medium conditions lead to the typical magnetospheric quiet-time periods during the analyzed days. The magnetopause standoff distance oscillated around 10 Earth radii and the solar wind dynamic pressure (about 1 nPa) shows a nondisturbed period. Also, the IMF *Bz* was not southwardly directed, suggesting the absence of the Earth's magnetic field reconnections. According to the Near-Earth Interplanetary Coronal Mass Ejections (ICME) Catalog, the solar wind did not drive any geomagnetic activity directed to Earth for the analyzed period (Cane & Richardson, 2003; Richardson & Cane, 2010, 2012). Therefore, the highlighted days refer to similar interplanetary medium and magnetospheric conditions.

2.2. The Geomagnetic Field Data

The ground-based geomagnetic field records are provided by magnetometer networks from Embrace Magnetometer Network (Embrace MagNet), Instituto Geofísico del Perú (IGP), and International Real-time Magnetic

Table 1
Magnetometer Locations, Including Quasi-Dipole Latitude (QDLAT), and Their Corresponding Information of First Contact Penumbra, Duration, and Maximum Obscuration

Location	Code	Geographic coordinate		QDLAT	Penumbra time (UT)	Duration (min)	Obs$_{max}$ (%)
		Latitude	Longitude				
San Juan	SJG	18.110°N	66.150°W	25.13°	–	–	–
Tatuoca	TTB	1.205°S	48.513°W	−1.46°	–	–	–
Piura	PIU	5.170°S	80.640°W	5.96°	14:15	90	6.62
Porto Velho	PVE	8.835°S	63.940°W	−0.58°	15:51	5	0.0004
Jicamarca	JIC	11.950°S	76.880°W	−0.67°	14:16	127	16.67
Jataí	JAT	17.932°S	51.718°W	−13.85°	15:45	130	12.96
Cachoeira Paulista	CXP	22.702°S	45.014°W	−20.84°	15:54	148	29.39
Medianeira	MED	25.300°S	54.114°W	−18.79°	15:20	164	36.73
São Martinho da Serra	SMS	29.444°S	53.823°W	−22.31°	15:17	172	52.38

Observatory Network (INTERMAGNET), with a 1-min resolution (Denardini et al., 2018a, 2018b; Love & Chulliat, 2013; Valladares & Chau, 2012).

The horizontal (*H*) component of the daily geomagnetic field variation is used to investigate the possible TSE effects. The average of the 5 (five) quietest days of the month, called the Quiet Day Curve (QDC), is shown to highlight the differences in the daily variation, as calculated by Chen et al. (2020). The daily variation amplitude is obtained by subtracting the baseline, that is, $\Delta H = H - H_0$, where ΔH is the geomagnetic field daily variation amplitude, *H* is the geomagnetic field daily variation magnitude, and H_0 is the magnetic field baseline given by an average of 23, 0, 1, and 2 hr in local time, according to Rabiu et al. (2007), that is, $H_0 = (H_{23} + H_0 + H_1 + H_2)/4$.

A list of magnetometers used in this analysis is presented in Table 1, in which data were selected during the solar eclipse and the control days. This table also shows the maximum obscuration (in percent) and solar eclipse penumbra duration (in minutes).

2.3. The TEC and RD Maps

We used the TEC maps to analyze the TSE effect in the ionosphere dynamics over South America. These maps are provided by the Embrace Program (http://www2.inpe.br/climaespacial/SWMonitorUser/). They are based on the data collected by the GNSS network receivers from Brazilian Network for Continuous Monitoring (IBGE/RBMC), International GNSS Service (IGS), Low Latitude Ionospheric Sensor Network (LISN), and Red Argentina de Monitoreo Satelital Continuo (RAMSAC). The Embrace TEC maps have a spatial resolution of 0.5° latitude per 0.5° longitude and 10 min of temporal resolution. Refer to Takahashi et al. (2016) for more information on the TEC calculation procedure. We also used the Relative Difference (RD) to calculate the difference between the evaluated TEC map and a reference TEC map. These RD maps have the same temporal and spatial resolution as the Embrace TEC maps. The RD is calculated by:

$$RD = \frac{TEC_{ecl} - TEC_{ref}}{TEC_{ref}} \times 100\% \tag{1}$$

where TEC_{ecl} and TEC_{ref} are the vertical TEC, in TEC units (1 TECu = 10^{16} electrons/m^2), during the eclipse day and the control day (or reference day), respectively. RD is the relative difference between the TEC_{ecl} and the TEC_{ref} (Resende et al., 2022).

3. Results and Discussions

3.1. The Solar Eclipse Effects on Ionospheric Currents

Figure 2 shows the daily variation of the ΔH (left axis) over (a) San Juan—SJG, (b) Jataí—JAT, (c) Cachoeira Paulista—CXP, (d) Medianeira—MED, and (e) São Martinho da Serra—SMS, representing the geomagnetic field variations of low latitude in the American sector. Each panel shows the geomagnetic field records on 14

(red) and 17 (orange) December 2020, the average of quiet days (blue) with ±1 standard deviation (blue shaded area), and the obscuration (magenta) in the right axis. Notice that the SJG station (Quasi-Dipole coordinate 25.13°N, 11.61°E) is the only Northern hemisphere magnetic data available on the eclipse day, which is almost the exact magnetic conjugate latitude of the SMS station (Quasi-Dipole coordinate 22.31°S, 13.06°E).

It is possible to verify in Figure 2 that the obscuration peak at JAT, CXP, MED, and SMS is 12.96%, 29.39%, 36.73%, and 52.38%, respectively. Note that the solar eclipse penumbra did not pass through SJG. In the Southern hemisphere, the higher discrepancies in the ΔH between the TSE day and reference conditions occurred in MED and SMS, stations with the maximum obscuration peaks. In such cases, we observe a reduction in the horizontal field intensity of ~15.77 and 13.36 nT over SMS and MED, respectively, around the eclipse hours compared to the reference day, despite the variation remaining close to ±1 σ of quiet condition. The reduction was ~11.22 and ~12.49 nT over CXP and JAT stations.

We noticed that the ΔH reduction started before the solar penumbra passes MED and SMS stations. The reduction approximately 15 nT on the horizontal component occurred ~1 and 2 hr earlier the solar penumbra reaches MED and SMS, respectively, and lasted until the last contact of the eclipse in these regions. Dang et al. (2018) simulated a similar global response of electric field/plasma drift during the solar eclipse event due to the global closure of the ionospheric current. They concluded that electrodynamic processes play an important role in the global responses of the ionosphere-thermosphere system during the solar eclipse event. In other words, even if the solar eclipse did not reach the region locally, there may be changes in parameters such as electric field and plasma drift due to the global closure of the ionospheric current since the solar eclipse has already passed in other regions. This can help us to understand the ΔH reduction over MED and SMS stations in the hours before the solar eclipse occurrence.

Conversely, we observe a peak of ~10.72 nT compared to the reference day at SJG, which is a magnetic conjugate point of SMS. This observation shows that the conjugate hemisphere was significantly changed during the eclipse day compared to the solar eclipse path observations. Notice that QDC in SJG had much lower values and with the contrary behavior compared to SMS. We believe that this fact may be evidence that one region is trying to compensate the other. Therefore, a peak in the H component maybe is related to the changes in the current which could be an eclipse effect. For instance, Takeda and Araki (1984) suggested that field-aligned currents flow to the opposite hemisphere to equal electrostatic potential between conjugate points. These authors regarded the existence of field-aligned currents during eclipses. Therefore, the solar eclipse events affect the conjugate hemisphere Sq current by deforming its current vortex. In addition, Liu et al. (2022) simulated a global effect of ionospheric current and ground geomagnetic variation. The authors found that there was a reduction concerning the 5 quiet days average in all components of the geomagnetic field during the time of eclipse obscuration, which depends on local time and latitude. Their results with simulations also show that in the conjugate points in the southern hemisphere, where the solar eclipse does not pass, the ionospheric currents were affected. They associated that these geomagnetic responses imply that the solar eclipse can reduce the Sq current system globally. Our work could not evaluate the Sq current shape of the Northern hemisphere due to the lack of low-latitude ground-based magnetometer measurements on 14 December 2020. Thus, future investigations with a larger amount of data from conjugate hemispheres are expected to evaluate better the solar eclipse effects in both hemispheres.

The solar eclipses induce conductivities reduction along the obscuration path as electron density is reduced due to the photoionization decrease. Since the electric conductivity can be modified, we analyzed the Equatorial Electrojet (EEJ) ground strength at the dip equator region during this event. Figure 3 shows the daily variation over Jicamarca (JIC), Porto Velho (PVE), and Tatuoca (TTB), the equatorial stations in South America. This figure shows the geomagnetic field variations during the eclipse day (red), the control day (orange), the average of quiet days (blue), and its standard deviation (blue shaded area). The obscuration percentage is also shown in magenta (right axis). It is important to mention that the low-latitude stations around the magnetic dip equator show different solar obscuration effects by the moon shadow path. First, the local daily variation records of the dip equator station are investigated to their corresponding obscuration.

In Jicamarca, the obscuration began at 14:16 UT and ended at 16:23 UT, reaching its peak (16.67%) at 15:15 UT. In this region, the geomagnetic field reduction reached about 52.33 nT at 17:21 UT and took 2 hr 50 m to recover to typical values. We did not observe any significant change in the geomagnetic field variation in the equatorial stations that the eclipse did not reach (PVE and TTB). This fact might be related to the fact that no eclipse penumbra reached these locations. Tomás et al. (2007) investigated the low-latitude and equatorial region effects of the
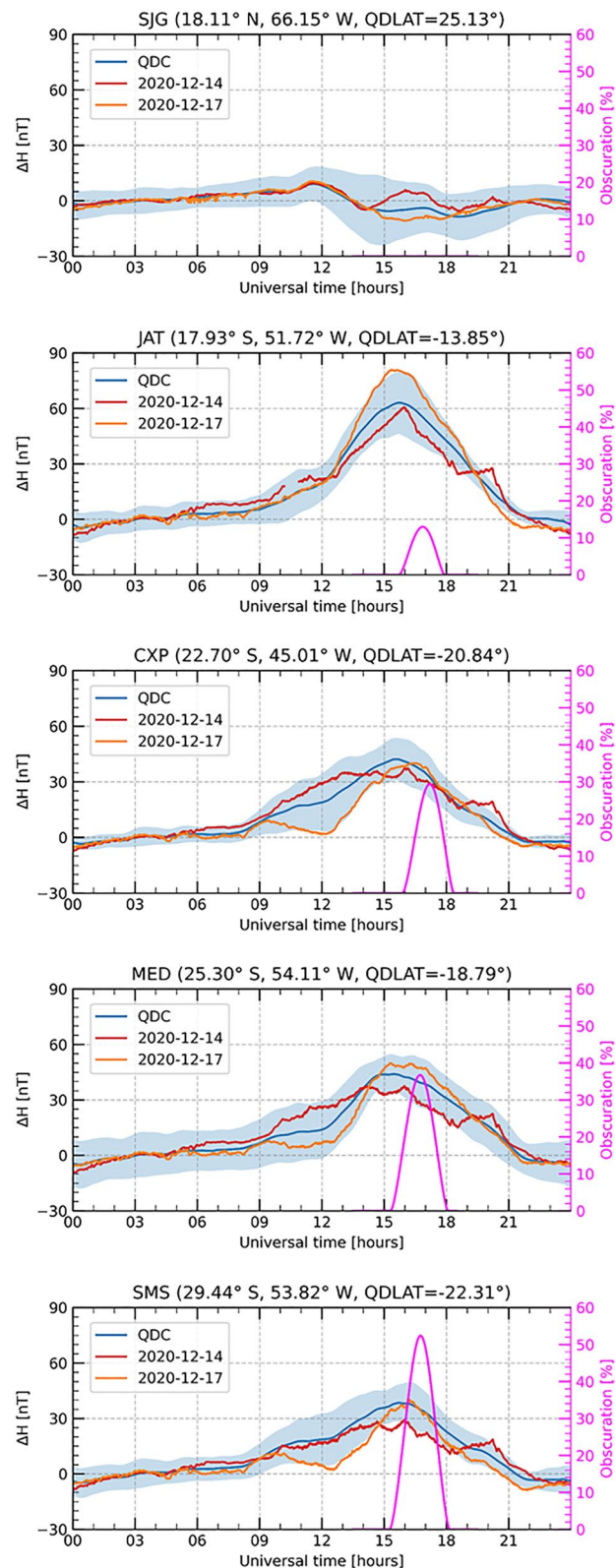
Figure 2. The ΔH variations (left axis) over the low-latitude stations of San Juan (SJG), Jataí (JAT), Cachoeira Paulista (CXP), Medianeira (MED), and São Martinho da Serra (SMS) on days 14 (red) and 17 (orange) December 2020. The QDC variation (blue) and its standard deviation (±1 σ, in blue shaded area), and the corresponding obscuration (magenta) (right axis) also is shown.
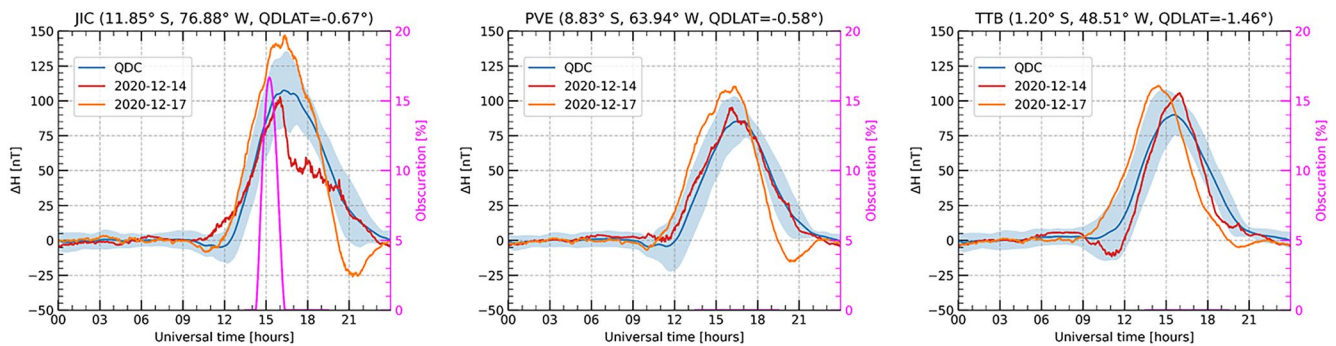
Figure 3. Same as Figure 2, but for the equatorial stations of Jicamarca (JIC), Porto Velho (PVE), and Tatuoca (TTB).

TSE on 8 April 2005 using CHAMP instrumentation. The authors observed an EEJ strength reduction of almost 40%. Tomás et al. (2008) studied the response of the EEJ strength during four TSEs, which occurred on 14 December 2001, 10 June 2002, 3 October 2005, and 29 March 2006. In those cases, the magnetic field records of satellites and ground-based observations were analyzed. Their results also show a local weakening of EEJ strength after the eclipse shadow passed the dip equator. The authors noted a reduction of about twice of expected variation on the ΔH of the magnetic records. Moreover, the Counter Electrojet (CEJ) was identified several minutes after the solar obscuration path reached its peak. St.-Maurice et al. (2011) analyzed the solar eclipse on 15 January 2010, crossing the magnetic equator at Trivandrum, India, in the early afternoon hours. They observed a strong CEJ was observed shortly after maximum obscuration. The CEJ did not occur in our case. However, Panda et al. (2015) suggest that the EEJ strength reversal on the eclipse day is not due to the solar eclipse but probably due to the strong gravitational tides. Our results show a clear local EEJ reduction during the TSE on 14 December 2020.

We calculated the EEJ ΔH using the stations in Jicamarca and Piura (5.17°S, 80.64°W, QDLAT = 5.96°) (Denardini et al., 2009), which is given by $\Delta H_{EEJ} = \Delta H_{JIC} - \Delta H_{PIU}$, where ΔH_{EEJ} is the EEJ ground strength, and the ΔH_{JIC} and ΔH_{PIU} are the variations of the geomagnetic field horizontal component over Jicamarca and Piura, respectively, shown in the Supporting Information S1. In Figure S1a in Supporting Information S1, it was noticed that the ΔH_{EEJ} from 14:00 UT to 15:00 UT was approximately 5 nT higher than observed at the peak obscuration in Jicamarca at 15:15 UT compared to the eclipse day (red line) and the average of the 5 quiet days (blue line). Besides this slight reduction in the ΔH_{EEJ} at 15:15 UT (10:15 LT) on the eclipse day, a significant reduction (~30 nT) after the eclipse obscured Jicamarca at 16:45 UT (11:45 LT). This delay between the obscuration peak and a more accentuated decrease in the horizontal current is clearly noticed in Figure 3. This behavior agrees with the study performed by Aa et al. (2020), in which they analyzed the ionosphere's response to the annular solar eclipse on 26 December 2019, utilizing ground-based measurements. The authors found that the inhibition of EEJ (or weakened substantially) occurred after eclipse passage for an Indian equatorial station. To explain this delay, we follow the analysis presented by Goncharenko et al. (2018). The ionization and recombination processes are expected to be fast in the E region during the eclipse. Besides the ionospheric density and conductivities explicitly related to the horizontal currents, the density and conductivities appear to yield only a minor role in the EEJ weakening. Hence, we suggest that the EEJ response delay could be related with the atmospheric GW, which was induced by the solar eclipse. In Section 3.3, we bring the discussions of GW evidence in Jicamarca.

We noted that the reference day (17 December 2020) on the geomagnetic field variations shows a day-to-day variability, which in low-latitude regions the values are around the standard deviation of the average of 5 quietest days of the month (QDC). On the other hand, the variability of 17 December 2020 in the equatorial region shows a much larger day-to-day variability. Despite the differences noticed between the reference day and the QDC, the analysis carried out on geomagnetic data was strict to the first and last contact of the eclipse and along with the local eclipse obscuration path, in which the eclipse-induced effects were related to the geomagnetic variations.

3.2. The Solar Eclipse Effect in the Equatorial Ionization Anomaly (EIA)

To better observe the solar eclipse effect in the equatorial ionosphere, we used the methodology presented by Anderson et al. (2004) to obtain the drift velocity, and consequently, the electric field. They used a neural network to obtain the following relationship between the vertical drift velocity ($\mathbf{E} \times \mathbf{B}/B^2$) in the regions near the equator and the ΔH:

$$\mathbf{E} \times \mathbf{B}/B^2 = -1989.51 + 1.002\text{year} - 0.00022\text{DOY} - 0.0222F10.7 - 0.0282\,F10.7A - 0.0229Ap_{\text{daily}}$$
$$+ 0.0589Kp - 0.3661LT + 0.1865\Delta H + 0.00028\Delta H^2 - 0.0000023\Delta H^3$$
(2)

in which $\mathbf{E} \times \mathbf{B}/B^2$ is the vertical plasma drift velocity, the year is 2020, DOY is the day of the year, which is 349 for December 14 (the eclipse day) and 352 for December 17 (the reference day), F10.7 is the daily solar radio flux in solar flux units (s.f.u.), F10.7 A is the monthly solar radio flux in s.f.u., Ap_{daily} is the daily Ap index, Kp is the 3-hr Kp index, LT is the local time, and ΔH is the EEJ ground strength obtained by Jicamarca minus Piura stations. The zonal electric field was obtained using the following relation: 40 m/s of the vertical drift velocity is equal to 1 mV/m, that is, $E = 40$ [m/s] $\propto$ 1 [mV/m] (Fejer & Scherliess, 1995).

The results of the vertical plasma drift velocity and the zonal electric fields are shown in Table 2, and the graphs of the vertical plasma drift and electric field are shown in the Supporting Information S1. It is possible to notice a clear reduction in these parameters after the maximum obscuration that lasts a long period (after 11 UT). This analysis indicates that the solar eclipse can reduce the Sq current system, and affect the ionosphere as a whole. Finally, in the next section, we discuss how this phenomenon affected the ionospheric dynamics on this day.

Figure 4 shows a quick overview of the TEC maps during four consecutive hours (15:30, 16:30, 17:30, and 18:30 UT) on (a) 14 and (b) 17 December 2020, and (c) the RD map. The EIA crest over the American Southern hemisphere is observed in the TEC red regions, meaning an electron density is concentrated around ∼−15° magnetic latitude of the magnetic equator (Takahashi et al., 2016). The eclipse obscuration contours are shown every 10% in black isoline. The Quasi-Dipole latitudes obtained from apex is shown for −30° to 30°, every 10° (red isolines) (Emmert et al., 2010). Stars indicate magnetometer sites, and the gray region is the nonsunlit area.

We observe that the ionospheric plasma density changes as the solar eclipse passes. The solar eclipse obscuration is expected to reduce the solar radiation over the eclipse path (Bravo et al., 2020; Cherniak & Zakharenkova, 2018; Coster et al., 2017; Eisenbeis & Occhipinti, 2021; Shrivastava et al., 2021). As some authors suggested (Bravo et al., 2020), ionospheric plasma production starts to increase after the last solar eclipse contact happens. In fact, the solar eclipse causes a local electron density modification. However, our results show two interesting behaviors. First, there was a significant reduction on the southern EIA crest (∼−20° QD latitudes) along the eclipse path but with a long duration after the solar eclipse passage. Second, we also observed a TEC reduction in the equatorial region, where the solar eclipse did not reach (between PVE and TTB). The RD maps show a maximum reduction of ∼10%–30% in the Southern crest of EIA.

Similar results of this solar eclipse event were recently reported by Resende et al. (2022). The authors did not show clear evidence of what caused the TEC reduction. They associated that the TEC reduction in the Southern crest is a local dynamic process of the loss-production of the photoionization. They also mentioned a possible plasma movement on the flux tube modifying the equatorial fountain effect. Additionally, Martínez-Ledesma et al. (2020) predicted a reduction of about 4.5 TECu along the totality eclipse path and a modification of up to 1.5 TECu on the conjugate hemisphere. However, both Resende et al. (2022) and Martínez-Ledesma et al. (2020) did not consider that this event largely reached the equatorial region of Jicamarca.

The abrupt decrease in the eastward EEJ ground strength during the solar eclipse hours can contribute to a reduction in the TEC of EIA crests besides the local effect. In fact, we believe that the TEC depletion in the EIA can be associated with variations in the equatorial electric field, neutral winds, and pressure parameters, which can also modify the fountain effect, causing changes the EIA crests. As observed in Figure 3, the EEJ strength weakens during solar obscuration at Jicamarca, indicating a localized solar eclipse effect at the dip equator. The other dip equator stations show changes in the EEJ strength in the maximum 5%–10%, meaning that, in general, the eastward electric field remains similar to its typical quiet conditions. Thus, the E region dynamo electric field should be reduced assuming that the longitude-integrated or solar-local-time-integrated electric fields along a latitude circle due to its divergence-free nature. The EIA is an important phenomenon of the equatorial and low-latitude ionosphere formed by upward vertical plasma drift $(\mathbf{E} \times \mathbf{B})/B^2$

Table 2
The Vertical Drift Velocity and the Zonal Electric Field in Jicamarca Are Derived Empirically From Anderson et al. (2004) and Fejer and Scherliess (1995), Respectively

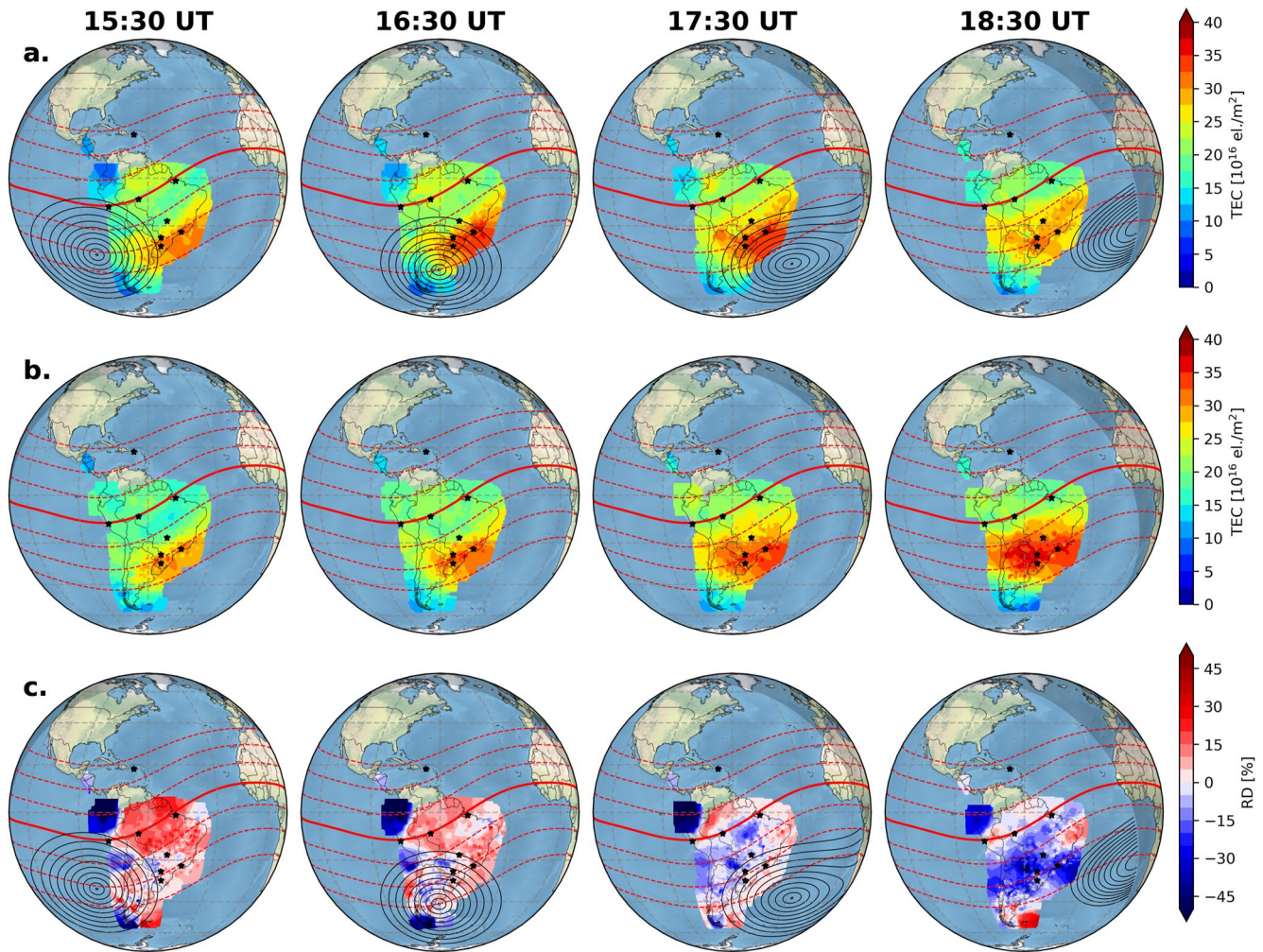| LT (hr)	UT (hr)	(E × B)/B² drift (m/s)			E (mV/m)		
		Anderson et al. (2004)			Fejer and Scherliess (1995)		
		Reference day	QDC	Eclipse day	Reference day	QDC	Eclipse day
9	14	34.1	30.4	31.7	0.852	0.760	0.792
10	15	38.4	34.7	35.5	0.959	0.867	0.887
11	16	40.4	36.1	37.1	1.010	0.903	0.927
12	17	38.6	35.2	30.1	0.966	0.880	0.752
13	18	35.7	33.6	30.4	0.892	0.841	0.759
14	19	29.7	31.8	30.0	0.743	0.794	0.751
15	20	23.1	29.3	30.2	0.577	0.733	0.756

Figure 4. Total Electron Content (TEC) maps on (a) 14 and (b) 17 December 2020, and the corresponding (c) RD map, from 15:30 UT to 18:30 UT, every 1 hr (left to right panels). Black isolines contours show the solar eclipse obscuration every 10%. Red isolines indicate the Quasi-Dipole latitudes from −30° to 30°, every 10°. Stars indicate the magnetometer sites.

that moves the ionospheric plasma to higher altitudes. Due to the diffusion process along the geomagnetic field lines and under the action of gravitational and pressure gradient forces, the plasma is removed from the equator creating a depletion of plasma over this region and ionization peaks/crests in the northern and southern hemispheres. However, as mentioned by Abdu et al. (1991), the EIA development occurs under the action of the E layer tide-induced dynamo electric field. Therefore, any change in the zonal electric field of the E region, as those decreases observed in the EEJ on 14 December 2020 over Jicamarca, will affect the plasma fountain effect (Balan & Iyer, 1983; Chen et al., 2008; Venkatesh et al., 2015). In this context, we suggest that the EEJ strength reduction during the TSE was responsible for the weakening of vertical drift velocity/zonal electric field, and consequently, the weakening of EIA development. Thus, the EEJ strength reduction explains the reduction of the TEC observed in the EIA crest on the eclipse day. Consequently, this behavior affected the equatorial plasma fountain effect and the EIA crests (Rama Rao et al., 2006; Venkatesh et al., 2015).

Aa et al. (2020) analyzed the TEC and EIA responses to the solar eclipse event on 26 December 2019 in Indian equatorial latitudes and Asian longitude sectors. Their results show a TEC depletion of up to 6 TECu (50%) in equatorial stations, which agrees with our results and those presented in Resende et al. (2022). Furthermore, the TEC has a longer recovery period when the solar eclipse passage occurs in the morning, leading to around 3 hr to return the reference values. According to the authors, one factor that contributed to this behavior is that the geomagnetic conditions are not so quiet during the morning. Another important observation in Aa et al.'s (2020)

work is a considerable EIA crest enhancement in the stations where solar eclipse passage occurred at midday. The authors show that both northern and southern EIA crests exhibited an increase of ∼20%–40%. They concluded that a combination of eclipse-induced electric field and neutral wind changes, added to the possible day-to-day ionospheric variability, contributed both to the enhancement and prolonged EIA crests. However, they mentioned that future numerical simulation analyses are necessary to comprehend this behavior better. In fact, we did not observe an EIA enhancement in our case.

Another interesting observation is the EIA crest weakening duration, mainly in the South. Notice that the TEC remains reduced after the solar eclipse passage (18:30 UT), around ∼5 TECu lower in the Southern crest. Deshpande et al. (1977) have reported the EEJ effects on the TEC over the Indian sector. They suggested that the electric field reversal causes downward drift motion at the magnetic equator, then the movement of ionization along magnetic field lines to 15°–20° magnetic latitude becomes ineffective. The authors also mentioned that the electron density returns to typical values after hours due to recombination factor delay during the solar eclipse. Here, the effects in the EIA crest are noticed ∼2–3 hr after the solar eclipse shadow. The EEJ in Jicamarca only returned to typical values 2 hr 50 m later.

Studies of the solar eclipse effect on the EIA show that it is not just the equatorial electric field that causes some modification in the plasma density (Dang et al., 2020; Huang et al., 2020). Dang et al. (2020) showed the different changes in the EIA southern and northern crests during the analysis of the solar eclipse passage from Africa to Southeast Asia on 21 June 2020. The authors affirm that the eclipse-induced temperature and pressure gradient variation can produce the TEC enhancement. In addition, they state that there is a difference between the TEC in EIA crests because of the neutral wind perturbations. They observed a decrease in the southern EIA crest, while in the northern crest the TEC enhanced. The same solar eclipse event was studied by Huang et al. (2020) in the East Asian sector. In this case, it was mentioned that the TEC depletion cannot solely be explained by the solar flux changes associated with the obscuration rate, as proposed by Resende et al. (2022). They suggested that the neutral winds driven by the eclipse play a dominant role in modifying the ionospheric variations. Thus, these disturbances in the neutral winds converge toward the eclipse totality, corroborating to the TEC reduction.

In our study, we believe that the maximum obscuration of 16.6% in Jicamarca induced enough attenuation of EUV solar irradiation, inhibiting in this way the equatorial electrodynamics and, consequently, affect the EIA Southern crest. It is important to mention that we observed the combined effect of the solar eclipse in the Southern crest. One of them is the local loss ionization reported by Resende et al. (2022), and another is the equatorial conductivity weakening observed in this work.

3.3. Other Ionospheric Dynamic Changes Caused by the Solar Eclipse in Jicamarca

The gradient drift instabilities (or Type II irregularities) due to the EEJ occurrence are observed in ionograms as type "q" sporadic E (Es) layers (Es_q) (Moro et al., 2017; Resende et al., 2013). These Es layers are characterized by diffuse, tinny, and non-blanketing traces in ionograms, occurring around 90–120 km altitude. Since the Es_q layer is related to the EEJ presence, any change in the EEJ behavior could affect this plasma instability.

Figure 5 shows a snapshot of the Vertical Incidence Pulsed Ionospheric Radar (VIPIR) ionograms on the eclipse day at three different times in Jicamarca. We observed the Es_q layer weakening at the onset time of EEJ decrease. The top to bottom panels show ionograms before (13:00 UT), during (14:38 UT), and after (17:31 UT) the solar eclipse shadow passed. Note that there is a clear Es_q layer weakening at 100 km height in the eclipse hours (white arrow) that did not recover to the previous scenario. The Signal-Noise-Ratio (SNR) strained from 40 to 10 dB during the eclipse and did not recover to higher than 20 dB after the solar eclipse passage. This Es_q layer weakening disagrees with the results in Pezzopane et al. (2015). The authors observed that the solar eclipse did not affect the Es layer in terms of its maximum intensity, which is comparable with that of the previous and next day. However, they analyzed the blanketing Es layers (Es_b), which has a different concept since the Es_b layer is produced by the electron density enhancements caused by tidal winds (Piggott & Rawer, 1978). Resende et al. (2022) also analyzed the Es_b layer changes in low-latitude stations in Brazil on 14 December 2020. The authors verified an increase in the sporadic E layer electron density and associated this with the strengthening of the GWs during the eclipse path.

Over the equatorial regions, Rastogi et al. (1971) reported a case study where the Es layer temporarily disappeared during the EEJ current reversal. It was suggested that during relatively quiet conditions and without
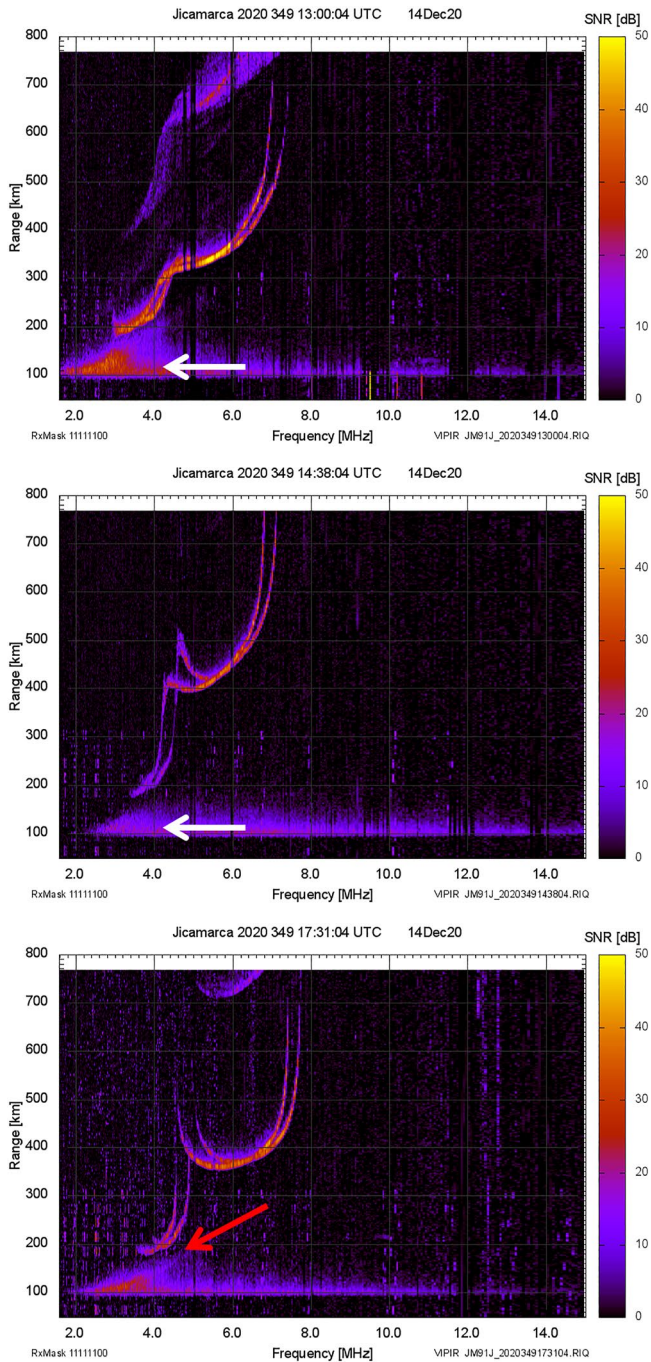
Figure 5. Vertical Incidence Pulsed Ionospheric Radar (VIPIR) ionograms before (13:00 UT), during (14:38 UT), and after (17:31 UT) the Total Solar Eclipse (TSE) shadow passed Jicamarca on 14 December 2020.

solar wave disturbances, an electric field with the opposite direction of the ambient Sq field reversed the currents and caused the Es layer disruption. Here, we hypothesize that the eclipse may have generated a disturbance in the ionosphere, decreasing the EEJ intensity. Thus, the typical eastward electric field was modified in the dayside equatorial ionosphere, and, consequently, the plasma irregularities were weaker, impacting the Es_q layer development.

It is possible to observe in Figure 5 a clear inclined trace at 17:31 UT (red arrow) in Jicamarca, which can be classified as another Es layer type known as the slant sporadic type (Es_s). The Es_s layer refers to the radio signal oblique propagation and is common in equatorial regions (Conceição-Santos et al., 2019). They can be associated with the presence of GWs embedded in the *E* layer (Cohen et al., 1962). Therefore, the GWs can have a significant role in the ionospheric changes during this solar eclipse event, as reported by Resende et al. (2022). The intensification of the GWs also seems to cause an influence in the higher heights, reaching the F region.

Figure 6 shows a set of nine selected ionograms of VIPIR ionosonde located in Jicamarca from 16:24 to 16:40 UT on 14 December 2020. As can be seen at 16:26 UT, the VIPIR ionosonde registered an ionospheric perturbation between ∼600 and 700 km and ∼6–7 MHz (see the white arrow). The following ionograms show this ionospheric perturbation propagating up to the base of the F2 layer at ∼400 km and ∼5 MHz. It is interesting to note an additional stratification in the lower part of the F1 layer, as denoted by the white dashed arrow. Such stratification is also known as the F0.5 layer (see, e.g., Mridula et al. (2014); Mridula and Pant (2017)). We verified some ionograms before 16:24 UT (not shown here) and noted that this disturbance in the F1 layer base was already present, but it was intensified during the eclipse. As mentioned by Mridula et al. (2014), the F0.5 layer can result from the variations in the amplitude and phases of the tides and GW. The observation lasted 16 min until no ionospheric perturbation was noticed afterward. This ionospheric perturbation shows a downward atmospheric GW propagating several minutes after the eclipse penumbra.

Lastly, in the equatorial region of Jicamarca, a TSE can significantly affect ionospheric dynamics. Our results support that the GWs were intensified during the solar eclipse event, causing the Es_s layer and the perturbation in the F region. We also believe that the changes in the Es_q layer characteristics, such as its intensity over Jicamarca, are concrete evidence of the weakening in the eastward electric field, which is a precursor of the gradient drift instability. Since an ionization reduction of at least 15% occurred in the E region (Resende et al., 2022), the dynamics affected the EEJ current and its irregularities.

4. Concluding Remarks

We analyzed the equatorial and low-latitude geomagnetic field records on the 14 December 2020 TSE with different obscuration magnitudes in South America. We have also reported ionospheric effects on the equatorial fountain effect caused by the partial eclipse obscuration on the western American sector.

First, in the low-latitude stations around the eclipse hours in the Southern hemisphere, we observed a reduction of ∼10–15 nT in the horizontal field intensity compared to the reference day. This geomagnetic field reduction is apparently due to a change in the E region conductivity caused by the ionization decrease during the eclipse event since the ionospheric production is affected. Conversely, a reduction of ∼10 nT compared to the reference
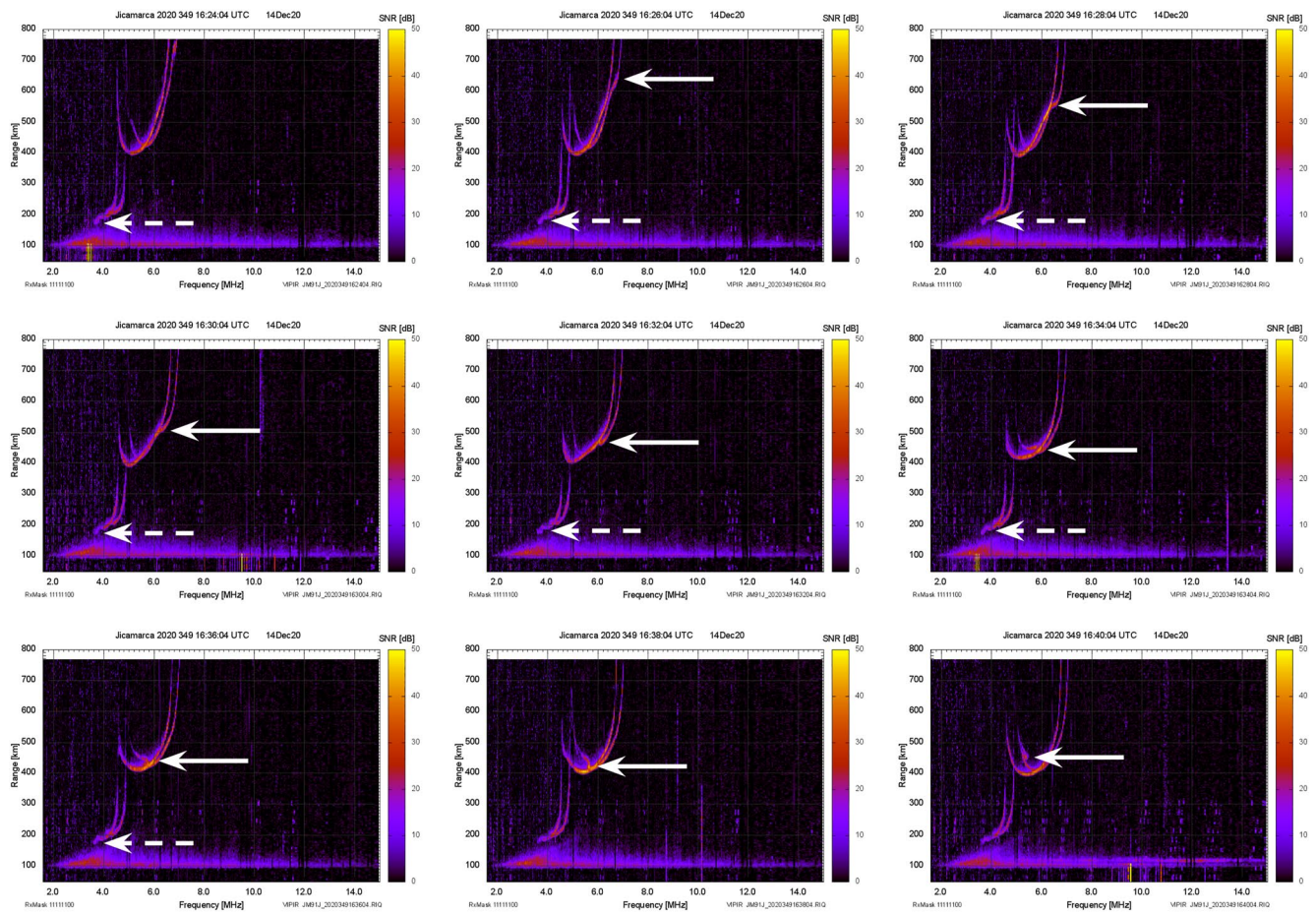
Figure 6. Vertical Incidence Pulsed Ionospheric Radar (VIPIR) ionograms from 16:24 to 16:40 UT on 14 December 2020 over Jicamarca.

day at SJG was noted, which is a magnetic conjugate point of SMS. This observation shows that the conjugate hemisphere was changed during the eclipse day. The field-aligned currents could be flowing from the Northern to the Southern hemisphere to keep electrostatic potential equal between conjugate points during the solar eclipse. However, we could not evaluate the Sq current shape to the Northern hemisphere due to the lack of low-latitude ground-based magnetometer measurements to this TSE.

We have noticed a local change in the EEJ strength at Jicamarca right after the eclipse shadow passed the dip equator. The EEJ weakened several minutes after the obscuration peak and took about ~2 hr 50 m to recover to its regular variation. The eclipse passing through Jicamarca apparently triggered the reduction in the behavior of the vertical drift velocity and its plasma fountain effect on the eclipse day, contributing to the EIA reduction. We believe that the E region dynamo electric field average was responsible for the decrease in the $\mathbf{E} \times \mathbf{B}$ vertical drift velocity and affected the EIA crest development uniformly. In this case, we considered that the E region dynamo electric field should be reduced if assuming the time-integrated electric field value over 24 hr. The combined effect of the local loss ionization and the equatorial conductivity weakening at Jicamarca possibly inhibited the equatorial electrodynamics.

Finally, the presence of GWs in Jicamarca caused the Es_s layer formation and produced a perturbation in the F region, as confirmed by the VIPIR ionograms. This perturbation could cause the formation of an additional stratification in the lower part of the F1 layer, also known as the F0.5 layer, that was intensified during the eclipse. The F0.5 layer can result from the variations in the amplitude and phases of the tides and GWs over Jicamarca. Furthermore, the Es_q layer changes over Jicamarca are concrete evidence of the weakening in the eastward electric field, which is a precursor of the gradient drift instability. Therefore, this analysis helped us understand how the solar eclipse can affect ionospheric dynamics in the equatorial region, even in locations not obscured by the eclipse.

Data Availability Statement

The magnetometer data are available online at the Embrace MagNet (http://www.inpe.br/climaespacial/Space-WeatherDataShare/), IGP/LISN (http://lisn.igp.gob.pe/jdata/database/), and INTERMAGNET (ftp://ftp.seismo.nrcan.gc.ca/intermagnet/) repositories. The TEC maps are available online at the Embrace website. The VIPIR ionogram data are available online in the LISN database.

References

Aa, E., Zhang, S. R., Erickson, P. J., Goncharenko, L. P., Coster, A. J., Jonah, O. F., et al. (2020). Coordinated ground-based and space-borne observations of ionospheric response to the annular solar eclipse on 26 December 2019. *Journal of Geophysical Research: Space Physics*, *125*, e2020JA028296. https://doi.org/10.1029/2020JA028296

Abdu, M. A., Sobral, J. H. A., de Paula, E. R., & Batista, I. S. (1991). Magnetospheric disturbance effects on the equatorial ionization anomaly (EIA): An overview. *Journal of Atmospheric and Terrestrial Physics*, *53*(8), 757–771. https://doi.org/10.1016/0021-9169(91)90126-R

Anderson, D., Anghel, A., Chau, J., & Veliz, O. (2004). Daytime vertical E × B drift velocities inferred from ground-based magnetometer observations at low latitudes. *Space Weather*, *2*, S11001. https://doi.org/10.1029/2004SW000095

Balan, N., & Iyer, K. N. (1983). Equatorial anomaly in ionospheric electron content and its relation to dynamo currents. *Journal of Geophysical Research*, *88*(A12), 10259–10262. https://doi.org/10.1029/JA088IA12P10259

Bauer, L. A. (1902). Results of international magnetic observations made during the total solar eclipse of May 18, 1901, including results obtained from previous total solar eclipses. *Terrestrial Magnetism and Atmospheric Electricity*, *7*(4), 155–192. https://doi.org/10.1029/TE007I004P00155

Bowhill, S. A. (1970). Ionospheric effects in solar eclipses. In M. Anastassiades (Ed.), *Solar eclipses and the ionosphere* (pp. 3–17). Springer. https://doi.org/10.1007/978-1-4684-1839-2_1

Bravo, M., Martínez-Ledesma, M., Foppiano, A., Urra, B., Ovalle, E., Villalobos, C., et al. (2020). First report of an eclipse from Chilean ionosonde observations: Comparison with total electron content estimations and the modeled maximum electron concentration and its height. *Journal of Geophysical Research: Space Physics*, *125*, e2020JA027923. https://doi.org/10.1029/2020JA027923

Cane, H. V., & Richardson, I. G. (2003). Interplanetary coronal mass ejections in the near-Earth solar wind during 1996–2002. *Journal of Geophysical Research*, *108*(A4), 1156. https://doi.org/10.1029/2002JA009817

Chapman, S. (1933). The effect of a solar eclipse on the Earth's magnetic field. *Terrestrial Magnetism and Atmospheric Electricity*, *38*(3), 175–183. https://doi.org/10.1029/te038i003p00175

Chapman, S., & Bartels, J. (1940). *Geomagnetism: Geomagnetic and related phenomena* (Vol. 1). Oxford University Press.

Chen, C. H., Liu, J. Y., Yumoto, K., Lin, C. H., & Fang, T. W. (2008). Equatorial ionization anomaly of the total electron content and equatorial electrojet of ground-based geomagnetic field strength. *Journal of Atmospheric and Solar-Terrestrial Physics*, *70*(17), 2172–2183. https://doi.org/10.1016/j.jastp.2008.09.021

Chen, S. S., Denardini, C. M., Resende, L. C. A., Chagas, R. A. J., Moro, J., & Picanço, G. A. S. (2020). Development of an empirical model for estimating the Quiet Day Curve (QDC) over the Brazilian sector. *Radio Science*, *55*, e2020RS007105. https://doi.org/10.1029/2020RS007105

Cherniak, I., & Zakharenkova, I. (2018). Ionospheric total electron content response to the great American solar eclipse of 21 August 2017. *Geophysical Research Letters*, *45*, 1199–1208. https://doi.org/10.1002/2017GL075989

Cohen, R., Bowles, K. L., & Calvert, W. (1962). On the nature of equatorial slant sporadic E. *Journal of Geophysical Research*, *67*(3), 965–972. https://doi.org/10.1029/JZ067i003p00965

Conceição-Santos, F., Muella, M. T. A. H., Resende, L. C. A., Fagundes, P. R., Andrioli, V. F., Batista, P. P., et al. (2019). Occurrence and modeling examination of sporadic- E layers in the region of the SouthSouth America (Atlantic) magnetic anomaly. *Journal of Geophysical Research: Space Physics*, *124*, 9676–9694. https://doi.org/10.1029/2018JA026397

Coster, A. J., Goncharenko, L., Zhang, S.-R., Erickson, P. J., Rideout, W., & Vierinen, J. (2017). GNSS observations of ionospheric variations during the 21 August 2017 solar eclipse. *Geophysical Research Letters*, *44*, 12041–12048. https://doi.org/10.1002/2017GL075774

Dang, T., Lei, J. H., Wang, W. B., Yan, M. D., Ren, D. X., & Huang, F. Q. (2020). Prediction of the thermospheric and ionospheric responses to the 21 June 2020 annular solar eclipse. *Earth and Planetary Physics*, *4*(3), 231–237. https://doi.org/10.26464/EPP2020032

Dang, T., Lei, J., Wang, W., Zhang, B., Burns, A., Le, H., et al. (2018). Global responses of the Coupled thermosphere and ionosphere system to the August 2017 great American solar eclipse. *Journal of Geophysical Research: Space Physics*, *123*, 7040–7050. https://doi.org/10.1029/2018JA025566

de Haro Barbás, B. F., Bravo, M., Elias, A. G., Martínez-Ledesma, M., Molina, G., Urra, B., et al. (2022). Longitudinal variations of ionospheric parameters near totality during the eclipse of December 14, 2020. *Advances in Space Research*, *69*(5), 2158–2167. https://doi.org/10.1016/j.asr.2021.12.026

Denardini, C. M., Abdu, M. A., Aveiro, H. C., Resende, L. C. A., Almeida, P. D. S. C., Olívio, Ê. P. A., et al. (2009). Counter electrojet features in the Brazilian sector: Simultaneous observation by radar, digital sounder and magnetometers. *Annales Geophysicae*, *27*(4), 1593–1603. https://doi.org/10.5194/angeo-27-1593-2009

Denardini, C. M., Chen, S. S., Resende, L. C. A., Moro, J., Bilibio, A. V., Fagundes, P. R., et al. (2018a). The Embrace magnetometer network for South America: First Scientific results. *Radio Science*, *53*, 379–393. https://doi.org/10.1002/2018RS006540

Denardini, C. M., Chen, S. S., Resende, L. C. A., Moro, J., Bilibio, A. V., Fagundes, P. R., et al. (2018b). The Embrace magnetometer network for south America: Network description and its qualification. *Radio Science*, *53*, 288–302. https://doi.org/10.1002/2017RS006477

Deshpande, M. R., Rastogi, R. G., Vats, H. O., Klobuchar, J. A., Sethia, G., Jain, A. R., et al. (1977). Effect of electrojet on the total electron content of the ionosphere over the Indian subcontinent. *Nature*, *267*(5612), 599–600. https://doi.org/10.1038/267599a0

Eisenbeis, J., & Occhipinti, G. (2021). TEC depletion generated by the total solar eclipse of 2 july 2019. *Journal of Geophysical Research: Space Physics*, *126*, e2021JA029186. https://doi.org/10.1029/2021JA029186

Emmert, J. T., Richmond, A. D., & Drob, D. P. (2010). A computationally compact representation of magnetic-apex and quasi-dipole coordinates with smooth base vectors. *Journal of Geophysical Research*, *115*, A08322. https://doi.org/10.1029/2010JA015326

Fejer, B. G., & Scherliess, L. (1995). Time dependent response of equatorial ionospheric electric fields to magnetospheric disturbances. *Geophysical Research Letters*, *22*(7), 851–854. https://doi.org/10.1029/95GL00390

Gómez, D. D. (2021). Ionospheric response to the 14 December 2020 total solar eclipse in South America. *Journal of Geophysical Research: Space Physics*, *126*, e2021JA029537. https://doi.org/10.1029/2021JA029537

Goncharenko, L. P., Erickson, P. J., Zhang, S. R., Galkin, I., Coster, A. J., & Jonah, O. F. (2018). Ionospheric response to the solar eclipse of 21 August 2017 in Millstone Hill (42) observations. *Geophysical Research Letters*, *45*, 4601–4609. https://doi.org/10.1029/2018GL077334

Huang, F., Li, Q., Shen, X., Xiong, C., Yan, R., Zhang, S. R., et al. (2020). Ionospheric responses at low latitudes to the annular solar eclipse on 21 June 2020. *Journal of Geophysical Research: Space Physics*, *125*, e2020JA028483. https://doi.org/10.1029/2020JA028483

Kato, Y. (1960). The effect on the geomagnetic of the solar eclipse of October 12,1958. *Science Reports of the Tohoku University*, *12*(1), 1–10.

Kim, J.-H., & Chang, H. Y. (2018). Geomagnetic field variations during solar eclipses and the geographic location of observing sites. *Journal of The Korean Astronomical Society*, *51*(4), 119–127. https://doi.org/10.5303/JKAS.2018.51.4.119

Korte, M., Lühr, H., Förster, M., Haak, V., & Bencze, P. (2001). Did the solar eclipse of August 11, 1999, show a geomagnetic effect? *Journal of Geophysical Research*, *106*(A9), 18563–18575. https://doi.org/10.1029/2001JA900006

Lepping, R. P., Acuña, M. H., Burlaga, L. F., Farrell, W. M., Slavin, J. A., Schatten, K. H., et al. (1995). The WIND magnetic field investigation. *Space Science Reviews*, *71*(1–4), 207–229. https://doi.org/10.1007/BF00751330

Liu, X., Chen, J., Han, P., Lei, J., Dang, T., Huang, F., et al. (2022). The response of geomagnetic daily variation and ionospheric currents to the annular solar eclipse on 21 June 2020. *Journal of Geophysical Research: Space Physics*, *127*, e2022JA030494. https://doi.org/10.1029/2022JA030494

Love, J. J., & Chulliat, A. (2013). An international network of magnetic observatories. *Eos, Transactions American Geophysical Union*, *94*, 373–374. https://doi.org/10.1002/2013EO420001

Martínez-Ledesma, M., Bravo, M., Urra, B., Souza, J., & Foppiano, A. (2020). Prediction of the ionospheric response to the 14 December 2020 total solar eclipse using SUPIM-INPE. *Journal of Geophysical Research: Space Physics*, *125*, e2020JA028625. https://doi.org/10.1029/2020JA028625

Meza, A., Bosch, G., Natali, M. P., & Eylenstein, B. (2021). Ionospheric and geomagnetic response to the total solar eclipse on 21 August 2017. *Advances in Space Research*, *69*, 16–25. https://doi.org/10.1016/j.asr.2021.07.029

Moro, J., Resende, L. C. A., Denardini, C. M., Xu, J., Batista, I. S., Andrioli, V. F., et al. (2017). Equatorial E region electric fields and sporadic E layer responses to the recovery phase of the November 2004 geomagnetic storm. *Journal of Geophysical Research: Space Physics*, *122*, 12517–12533. https://doi.org/10.1002/2017JA024734

Mridula, N., & Pant, T. K. (2017). On the role of horizontal wind shears in the generation of F0.5 layers over the dip equatorial location of Thiruvananthapuram: A numerical simulation study. *Journal of Atmospheric and Solar-Terrestrial Physics*, *155*, 79–85. https://doi.org/10.1016/j.jastp.2017.02.005

Mridula, N., Pant, T. K., Vineeth, C., & Kishore Kumar, K. (2014). Features of the occurrence of the additional stratification on the bottom-side F region over the equatorial location of Trivandrum. *Advances in Space Research*, *54*(3), 403–408. https://doi.org/10.1016/J.ASR.2013.12.036

Ogilvie, K. W., Chornay, D. J., Fritzenreiter, R. J., Hunsaker, F., Keller, J., Lobell, J., et al. (1995). SWE, a comprehensive plasma instrument for the WIND spacecraft. *Space Science Reviews*, *71*(1–4), 55–77. https://doi.org/10.1007/BF00751326

Orozco, A. L., & Muniz Barreto, L. (1993). Magnetic effects during the solar eclipse of July 11, 1991. *Geofísica Internacional*, *32*(1), 3–13. https://doi.org/10.22201/igeof.00167169p.1993.32.1.1147

Özcan, O., & Aydoğdu, M. (2004). Possible effects of the total solar eclipse of August 11, 1999 on the geomagnetic field variations over Elaziğ-Turkey. *Journal of Atmospheric and Solar-Terrestrial Physics*, *66*(11), 997–1000. https://doi.org/10.1016/J.JASTP.2004.03.009

Panda, S. K., Gedam, S. S., Rajaram, G., Sripathi, S., & Bhaskar, A. (2015). Impact of the 15 January 2010 annular solar eclipse on the equatorial and low latitude ionosphere over the Indian region. *Journal of Atmospheric and Solar-Terrestrial Physics*, *135*, 181–191. https://doi.org/10.1016/j.jastp.2015.11.004

Pezzopane, M., Pignalberi, A., & Pietrella, M. (2015). On the influence of solar activity on the mid-latitude sporadic E layer. *Journal of Space Weather and Space Climate*, *5*, A31. https://doi.org/10.1051/SWSC/2015031

Piggott, W. R., & Rawer, K. (1978). World Data Center A for solar-Terrestrial Physics. In W. R. Piggott, & K. Rawer (Eds.), *U.R.S.I. Handbook of ionogram interpretation and reduction* (2nd ed.). National Oceanic and Atmospheric Administration.

Rabiu, A. B., Mamukuyomi, A. I., & Joshua, E. O. (2007). Variability of equatorial ionosphere inferred from geomagnetic field measurements. *Bulletin of the Astronomical Society of India*, *35*, 607–618.

Rama Rao, P. V. S., Gopi Krishna, S., Niranjan, K., & Prasad, D. S. V. V. D. (2006). Temporal and spatial variations in TEC using simultaneous measurements from the Indian GPS network of receivers during the low solar activity period of 2004–2005. *Annales Geophysicae*, *24*(12), 3279–3292. https://doi.org/10.5194/ANGEO-24-3279-2006

Rastogi, R. G., Chandra, H., & Chakravarty, S. C. (1971). The disappearance of equatorial Es and the reversal of electrojet current. *Proceedings of the Indian Academy of Sciences*, *74*(2), 62–67.

Resende, L. C. A., Denardini, C. M., & Batista, I. S. (2013). Abnormal fb Es enhancements in equatorial Es layers during magnetic storms of solar cycle 23. *Journal of Atmospheric and Solar-Terrestrial Physics*, *102*, 228–234. https://doi.org/10.1016/j.jastp.2013.05.020

Resende, L. C. A., Zhu, Y., Denardini, C. M., Chen, S. S., Chagas, R. A. J., Da Silva, L. A., et al. (2022). A multi-instrumental and modeling analysis of the ionospheric responses to the solar eclipse on 14 December 2020 over the Brazilian region. *Annales Geophysicae*, *40*(2), 191–203. https://doi.org/10.5194/angeo-40-191-2022

Richardson, I. G., & Cane, H. V. (2010). Near-earth interplanetary coronal mass ejections during solar cycle 23 (1996–2009): Catalog and summary of properties. *Solar Physics*, *264*(1), 189–237. https://doi.org/10.1007/s11207-010-9568-6

Richardson, I. G., & Cane, H. V. (2012). Solar wind drivers of geomagnetic storms during more than four solar cycles. *Journal of Space Weather and Space Climate*, *2*, A01. https://doi.org/10.1051/swsc/2012001

Rishbeth, H. (1970). Eclipse effects in the ionosphere. *Nature*, *226*(5251), 1099–1100. https://doi.org/10.1038/2261099a0

Shrivastava, M. N., Maurya, A. K., & Kumar, K. N. (2021). Ionospheric perturbation during the South American total solar eclipse on 14th December 2020 revealed with the Chilean GPS eyeball. *Scientific Reports*, *11*(1), 1–13. https://doi.org/10.1038/s41598-021-98727-w

Shue, J.-H., Song, P., Russell, C. T., Steinberg, J. T., Chao, J. K., Zastenker, G., et al. (1998). Magnetopause location under extreme solar wind conditions. *Journal of Geophysical Research*, *103*(A8), 17691–17700. https://doi.org/10.1029/98JA01103

St.-Maurice, J. P., Ambili, K. M., & Choudhary, R. K. (2011). Local electrodynamics of a solar eclipse at the magnetic equator in the early afternoon hours. *Geophysical Research Letters*, *38*, L04102. https://doi.org/10.1029/2010GL046085

Takahashi, H., Wrasse, C. M., Denardini, C. M., Pádua, M. B., de Paula, E. R., Costa, S. M. A., et al. (2016). Ionospheric TEC weather map over South America. *Space Weather*, *14*, 937–949. https://doi.org/10.1002/2016SW001474

Takeda, M., & Araki, T. (1984). Ionospheric currents and fields during the solar eclipse. *Planetary and Space Science*, *32*(8), 1013–1019. https://doi.org/10.1016/0032-0633(84)90057-6

Tomás, A. T., Lühr, H., Förster, M., Rentz, S., & Rother, M. (2007). Observations of the low-latitude solar eclipse on 8 April 2005 by CHAMP. *Journal of Geophysical Research*, *112*, A06303. https://doi.org/10.1029/2006JA012168

Tomás, A. T., Lühr, H., Rother, M., Manoj, C., Olsen, N., & Watari, S. (2008). What are the influences of solar eclipses on the equatorial electrojet? *Journal of Atmospheric and Solar-Terrestrial Physics*, *70*(11–12), 1497–1511. https://doi.org/10.1016/J.JASTP.2008.05.009

Valladares, C. E., & Chau, J. L. (2012). The low-latitude ionosphere Sensor network: Initial results. *Radio Science*, *47*, RS0L17. https://doi.org/10.1029/2011RS004978

van der Laan, J. E. (1970). Ionospheric and magnetic observations during the annular solar eclipse of November 23, 1965. *Journal of Geophysical Research*, *75*(7), 1312–1318. https://doi.org/10.1029/JA075I007P01312

Venkatesh, K., Fagundes, P. R., Prasad, D. S. V. V. D., Denardini, C. M., de Abreu, A. J., de Jesus, R., & Gende, M. (2015). Day-to-day variability of equatorial electrojet and its role on the day-to-day characteristics of the equatorial ionization anomaly over the Indian and Brazilian sectors. *Journal of Geophysical Research: Space Physics*, *120*, 9117–9131. https://doi.org/10.1002/2015JA021307